Era3D: High-Resolution Multiview Diffusion Using Efficient Row-wise Attention

Peng Li[1*] **Yuan Liu**[2,3*] **Xiaoxiao Long**[1,2†] **Feihu Zhang**[3] **Cheng Lin**[2] **Mengfei Li**[1]

Xingqun Qi[1] **Shanghang Zhang**[4] **Wenhan Luo**[1] **Ping Tan**[1,5] **Wenping Wang**[2]

Qifeng Liu[1] **Yike Guo**[1†]

[*]Equal contribution [†]Corresponding author

[1]HKUST [2]HKU [3]DreamTech [4]PKU [5]LightIllusion

Abstract

In this paper, we introduce **Era3D**, a novel multiview diffusion method that generates high-resolution multiview images from a single-view image. Despite significant advancements in multiview generation, existing methods still suffer from camera prior mismatch, inefficacy, and low resolution, resulting in poor-quality multiview images. Specifically, these methods assume that the input images should comply with a predefined camera type, e.g. a perspective camera with a fixed focal length, leading to distorted shapes when the assumption fails. Moreover, the full-image or dense multiview attention they employ leads to a dramatic explosion of computational complexity as image resolution increases, resulting in prohibitively expensive training costs. To bridge the gap between assumption and reality, Era3D first proposes a diffusion-based camera prediction module to estimate the focal length and elevation of the input image, which allows our method to generate images without shape distortions. Furthermore, a simple but efficient attention layer, named row-wise attention, is used to enforce epipolar priors in the multiview diffusion, facilitating efficient cross-view information fusion. Consequently, compared with state-of-the-art methods, Era3D generates high-quality multiview images with up to a 512×512 resolution while reducing computation complexity of multiview attention by 12x times. Comprehensive experiments demonstrate the superior generation power of Era3D- it can reconstruct high-quality and detailed 3D meshes from diverse single-view input images, significantly outperforming baseline multiview diffusion methods. Project page: `https://penghtyx.github.io/Era3D/`.

1 Introduction

3D reconstruction from single-view images is an essential task in computer vision and graphics due to its potential applications in game design, virtual reality, and robotics. Early research [42, 44, 53, 78, 28] mainly relies on direct 3D regression on voxels [39, 58, 9], which often leads to oversmoothed results and has difficulty in generalizing to real-world unseen objects due to limited 3D training data [4]. Recently, diffusion models (DMs) [16, 50] show strong generation ability on image or video synthesis by training on extremely large-scale datasets [47, 48]. These diffusion models are promising tools for single-view 3D reconstruction because it is possible to generate novel-view images from the given image to enable 3D reconstruction.

38th Conference on Neural Information Processing Systems (NeurIPS 2024).

Figure 1: Given single-view image with arbitrary intrinsic and viewpoints, Era3D can generate high-quality multiview images with a resolution of 512×512 on the orthogonal camera setting, which can be used in mesh reconstruction by NeuS [68].

To utilize image DMs for single-view 3D reconstruction, a pioneer work DreamFusion [46] tries to distill a 3D representation like NeRF [36] or Gaussian Splatting [62] from a 2D image diffusion by a Score Distillation Sampling (SDS) loss and many follow-up works improve the distillation-based methods in quality [71] and efficiency [62]. However, these methods suffer from unstable convergence and degenerated quality. Alternatively, recent works such as MVDream [55], SyncDreamer [33], Wonder3D [34] and Zero123++ [54] explicitly generate multiview images by multiview diffusion [64, 33] and then reconstruct 3D models from the generated images by neural reconstruction methods [68] or large reconstruction models (LRMs) [19, 27]. Explicitly generating multiview images makes these methods more controllable and efficient than SDS methods and thus is more popular in the single-view 3D reconstruction task.

Despite impressive advancements in multiview diffusion methods [55, 34, 33, 32, 31, 64, 63, 27], efficiently generating novel-view images for high-quality 3D reconstruction remains an open challenge. There are three noticeable challenges in the current approaches. (1) **Inconsistent predefined camera type**. Most multiview diffusion methods assume that the input images are captured by a camera with a predefined focal length. This leads to unwanted distortions when input images are captured by cameras with different camera types or intrinsics, as exemplified in Fig. 2 (e.g., Wonder3D's assumption of an orthogonal camera leads to distorted meshes when the input image is captured by a perspective camera with a small focal length). (2) **Inefficiency of multiview diffusion**. Multiview diffusion methods usually rely on multiview attention layers to exchange information among different views to generate multiview-consistent images. However, these multiview attention layers are usually implemented by extending the self-attention in Stable

Figure 2: (top) Perspective input images for Wonder3D produce extreme distortion in the generation. (bottom) Era3D can handle images of commonly used intrinsics.

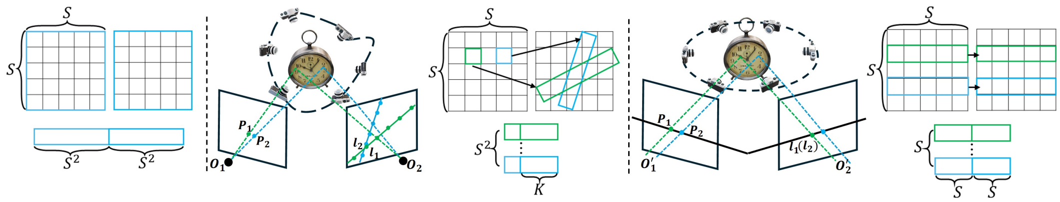

(a) Dense Attention $O(N^2S^4)$ (b) General Camera Setting (c) Epipolar Attention $O(N^2S^2K)$ (d) Canonical Camera Setting (e) Row-wise Attention $O(N^2S^3)$

Figure 3: Different types of multiview attention layers. (**a**) In a dense multiview attention layer, all feature vectors of multiview images are fed into an attention block. For a general camera setting (**b**) with arbitrary viewpoints and intrinsics, utilizing epipolar constraint to construct an epipolar attention (**c**) needs to correlate the features on the epipolar line. This means that we need to sample K points along each epipolar line to compute such an attention layer. In our canonical camera setting (**d**) with orthogonal cameras and viewpoints on an elevation of $0°$, epipolar lines align with the row of the images across different views (**e**), which eliminates the need to resample epipolar line to compute epipolar attention. We assume the latent feature map has a resolution of $H \times W$ and $H = W = S$. In such a N-view camera system, row-wise attention reduces the computational complexity to $O(N^2S^3)$.

Diffusion [52] to all multiview images, which is called dense multiview attention in Fig.3(a) and results in a significant increase in computation complexity and memory consumption. (3) **Low resolution of generated images**. The limitation above restricts most existing multiview diffusion models to resolutions of 256×256, preventing them from reconstructing detailed meshes. Addressing above challenges is crucial for developing practical and scalable multiview diffusion methods.

In this paper, we introduce Era3D, a novel multiview diffusion method that efficiently generates high-resolution (512×512) consistent-multiview images for single-view 3D reconstruction. Unlike existing methods, Era3D allows images of commonly used camera types as inputs while mitigating the unwanted distortion brought by different camera models.

To this end, we employ a unique approach: using different camera models for input images and the generated ones for training, meaning that the input images are allowed to have arbitrary focal lengths and elevations while generated images are with orthogonal cameras and fixed viewpoints of $0°$ elevations. However, this requires DMs to implicitly infer and rectify the focal lengths and viewpoints of input images in the generation process, which is a challenging task and degrades the generation quality. To overcome this challenge and improve generation quality, we propose a novel regression and condition scheme and utilize the low-level feature maps of UNet at each denoising step to predict camera information of input images. We find that such a regression and condition scheme facilitates much more accurate camera pose prediction than existing methods [31] and leads to more details in the generation. As shown in Fig. 2, Era3D successfully avoids the above distortion problem brought by the different camera types and focal lengths.

Moreover, drawing inspiration from epipolar attention [65], Era3D enables efficient training for high-resolution multiview generation by introducing a novel row-wise multiview attention. Epipolar constraint can be utilized to constrain the attention regions across views and thus improve attention efficiency. However, directly applying such epipolar attention [65] for a general camera setting (Fig. 3(b)) is still memory and computationally inefficient because one would have to sample multiple points on epipolar lines for attention. This would require to construct a 3D grid of features in the view frustums for multiview images, which is too slow and memory-consuming. In contrast, since Era3D generates images with orthogonal cameras on viewpoints of $0°$, we find that epipolar lines in our camera setting are aligned with pixel rows of images across different views (Fig. 3(d)), which enables us to propose an efficient row-wise attention layer. Compared with dense multiview attention, row-wise attention significantly reduces memory consumption (35.32GB v.s. 1.66GB), and the computation complexity (220.41ms v.s. 2.23ms) of multiview attention (Fig. 3(e)). Even with Xformers [26], an accelerating library for attention, the efficiency of row-wise attention still outperforms existing methods by approximately twelve-fold as evident in Tab. 3. Consequently, the proposed row-wise attention allows us to easily scale Era3D to a high resolution of 512×512 to reconstruct more detailed 3D meshes.

Overall, our main contributions are summarized as follows: (1) Era3D is the first method that tries to solve the distortion artifacts brought by the inconsistent camera intrinsic in 3D generation; (2) we design a novel regression and condition scheme to enable diffusion models to take images of arbitrary cameras as inputs while outputting the orthogonal images on the canonical camera setting; (3) we propose row-wise multiview attention, an efficient attention layer for high-resolution multiview image generation; (4) our method achieves state-of-the-art performance for single-view 3D generation [10].

2 Related Works

Our study is primarily centered on the domain of image-to-3D. Unlike early works [6, 49, 62, 71, 29], which concentrate on per-scene optimization based on Score Distillation Sampling [46, 67], we emphasize feed-forward 3D generation.

Image to 3D. Generating 3D assets from images has been extensively researched, paralleling the development of GAN [13, 23, 38] and diffusion models (DMs) [57, 17, 11, 18]. A stream of these works [20, 79, 5, 19, 76], directly produce 3D representations, like SDF [43, 9, 41], NeRF [36, 14, 1], Triplane [3, 15, 56], Gaussian [24, 59] or 3D volume [60]. Zero-1-to-3 [32] and subsequent works [54, 31] represent the scene as a diffusion model conditioned on reference image and camera pose. LRM-based methods [19, 27, 70, 74] employ a large transformer architecture to train a triplane representation with a data-driven approach. Another technical line involves generating consistent multiview images first [55, 69, 54, 72], and then robustly reconstructing 3D shapes with NeuS [33, 34], Gaussian Splatting [61, 19, 75] or LRM [73]. Despite significant advancements, challenges remain in reconstruction quality, training resolution, or efficiency.

Multiview diffusion. Cross-view consistency is critical in 3D reconstruction and generation, relying on multiview feature correspondence to estimate 3D structures. MVffusion [64] first proposes generating multiview images in parallel with correspondence-aware attention, facilitating cross-view information interaction, and applies to texture scene meshes. [65, 22] introduces epipolar features into DM to enhance fusion between viewpoints. Zero123++ [54] tiles multi-views into a single image and performs a single pass for multiview generation, which is also used in Direct2.5 and Instant3D. MVDream [55] and Wonder3D [34] also design multiview self-attention to improve multiview consistency. Syncdreamer [33] composes multiview features into 3D volumes, conducting 3D-aware fusion in 3D noise space. All of the aforementioned methods share the same idea: modeling 3D generation with multiview joint probability distribution. Other works [8, 66] explore the priors from video diffusion model to achieve consistent multiview generation. Following widely used multiview self-attention, we propose more efficient row-wise attention to reduce computation workloads, but without loss of multiview feature interaction.

Camera pose. For 3D generation, early works [32, 55] are trained with fixed focal lens. When inference, one also needs to provide elevation of input for better performance. Further research seeks to mitigate this issue by leveraging fixed poses [34, 54] or incorporating additional elevation prediction modules [30]. LEAP [20] uses pixel-wise similarity, rather than estimated poses, to aggregate multiview features. However, none of these methods consider the distortion error caused by cameras, which can severely affect the reconstruction of real-world data. To overcome this, we opt to generate images at fixed views in the canonical orthogonal space, with simultaneous predictions of elevation and focal distortion.

3 Methods

Era3D is proposed to generate a 3D mesh from a single-view image. The overview is shown in Fig. 4, consisting of three key components. Given an input image with commonly used focal length and arbitrary viewpoint, Era3D generates multiview images in a canonical camera setting as introduced in Sec. 3.1. To improve the generation quality, in Sec. 3.2, we propose a regression and condition scheme, enabling diffusion models to predict accurate camera pose and focal lengths and guiding the denoising process. Finally, we considerably reduce memory consumption and improve computation efficiency by proposing row-wise multiview attention (Sec. 3.3), which exchanges information among multiview images to maintain multiview consistency. Finally, we reconstruct the 3D mesh from the generated images and normal maps using neural reconstruction methods like NeuS [68].

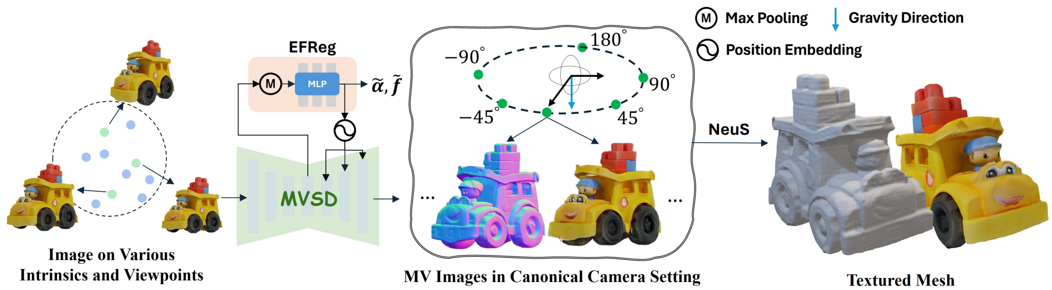

Figure 4: **Overview**. Given a single-view image as input, Era3D applies multiview diffusion to generate multiview consistent images and normal maps in the canonical camera setting, which enables us to reconstruct 3D meshes using NeuS [68, 37].

3.1 Camera Canonicalization

Perspective distortion problem. Existing multiview diffusion methods [33, 34, 54, 32] assume that the input image and the generated images share the same fixed intrinsic parameters. However, this assumption is often violated in practice, as input images may be captured by arbitrary cameras with varying focal lengths. When the input image has a different intrinsic matrix from the assumed one, the generated multiview images and reconstructed 3D meshes will exhibit perspective distortion, as illustrated in Fig. 2. This issue arises because these models are trained on renderings of the Objaverse [10] dataset with a fixed intrinsic and thus these models are severely biased towards the geometry patterns present in this fixed intrinsic matrix.

Canonical camera setting. To address this problem, Era3D uses different intrinsic parameters for input and generated images. Regardless of the focal length and pose of the input image, we consistently generate orthogonal images with an elevation of 0°. For example, when processing an input image captured at elevation α and azimuth β, Era3D produces a set of multiview images at an azimuth of $\{\beta, \beta + 45°, \beta + 90°, \beta - 45°, \beta - 90°, \beta + 180°\}$ and an elevation of 0°. We refer to the setup of these output images as a *Canonical* camera setting.

3.2 Regression and Condition Scheme

Given an image with an arbitrary viewpoint and focal length, generating novel-view images in the canonical camera setting is challenging because this implicitly puts an additional task on the diffusion model to infer the focal lengths and elevation of the input image. To make it easier, previous methods [32, 33, 2] rely on additional elevation inputs or predictions as the conditions for the diffusion model. However, pose estimation from a single image is inherently ill-posed due to the lack of geometry information. Moreover, even though estimating a rough elevation is possible, it is almost impossible for users to estimate the focal length of the input image.

To address this problem, we propose incorporating an Elevation and Focal length Regression module (**EFReg**) into the diffusion model. We use the feature maps of UNet to predict the camera pose in the diffusion process. Our motivation stems from the fact that the feature maps of UNet not only contain the input images but also include the current generation results which provide richer and more informative features for predicting the camera pose.

Specifically, within the middle-level transformer block of the UNet, we apply global average pooling to the hidden feature map $\mathbf{H}$, yielding a feature vector that is subsequently fed into three Multilayer Perceptron (MLP) layers $\mathcal{R}_1$ and $\mathcal{R}_2$ to regress the elevation $\tilde{\alpha}$ and focal lens $\tilde{f}$

$$\tilde{\alpha} = \mathcal{R}_1(\text{AvgPool}(\mathbf{H})), \tilde{f} = \mathcal{R}_2(\text{AvgPool}(\mathbf{H})). \tag{1}$$

The regressed elevation $\tilde{\alpha}$ and focal length $\tilde{f}$ are supervised by the ground-truth elevation α and focal length f by

$$\ell_{\text{regress}} = \text{MSE}(\tilde{\alpha}, \alpha) + \text{MSE}(\tilde{f}, f). \tag{2}$$

Then, the regressed $\tilde{\alpha}$ and $\tilde{f}$ are used as conditions in the diffusion process. We apply positional encoding on $\tilde{\alpha}$ and $\tilde{f}$ and concatenate them with the time embeddings of the Stable Diffusion model.

The concatenated feature vectors are used in all the upsampling layers of the UNet, providing information about the estimated focal lengths and elevations for better denoising.

3.3 Row-wise Multiview Attention (RMA)

To generate multiview-consistent images, multiview diffusion models typically rely on multiview attention layers to exchange information among generated images. Such layers are often implemented by extending the existing self-attention layers of Stable Diffusion to conduct the attention on all the generated multiview images [34, 55, 69, 63]. However, this dense multiview attention can be computationally expensive and memory-intensive, as it processes all pixels of all multiview images. This limitation hinders the scalability of multiview diffusion models to high resolutions, such as 512×512.

Since the pixels of multiview images are related by epipolar geometry, considering epipolar lines in multiview attention could possibly reduce computational and memory complexity. However, strictly considering epipolar attention [65] in general two-view camera setting still consumes massive computation and memory. As shown in Fig. 3(b), for a pixel on camera O_1, we find its corresponding epipolar line in camera O_2 by the relative camera pose. Then, we need to sample K points on the epipolar lines to conduct cross attention between these sample points of O_2 and the input pixel of O_1. In the following, we propose an efficient and compact row-wise multiview attention, which is a special epipolar attention tailored to our canonical camera setting.

In our canonical camera setting, cameras are distributed at an elevation of 0° around an object. Therefore, we can easily demonstrate the following proposition.

Proposition 1 *If two orthogonal cameras look at the origin with their y coordinate aligned with gravity direction and their elevations of $0°$ as shown in Fig. 3(d), then for a pixel with coordinate $(x, y) = (u, v)$ on one camera, its corresponding epipolar line on other views is $y = v$.*

We leave the proof in the supplementary material. Proposition 1 is a simplification of epipolar constraint, revealing that all epipolar lines correspond to rows in the generated multiview images. Building on this insight, we leverage the epipolar constraint by applying new self-attention layers on the same row across generated images to learn multiview consistency. By exploiting this constraint, we avoid the computational expense of dense multiview attention and instead accurately focus attention on epipolar lines. Moreover, our row-wise attention layer only involves elements from the same row, rather than sampling multiple points on the epipolar line, thereby significantly reducing computational complexity and facilitating training even on high-resolution inputs such as 512×512.

4 Experiments

Datasets. We trained Era3D on a subset of Objaverse [10]. To construct training images, we render 16 ground-truth images using orthogonal cameras with evenly distributed azimuth from 0° to 360° and a fixed elevation of 0°. Subsequently, for each azimuth, we render 3 more images using perspective cameras and one image using an orthogonal camera, both of which have random elevations sampled from the range $[-20, 40]$ degrees. The perspective camera has a focal length randomly selected from the set $\{35, 50, 85, 105, 135\}$ mm, which are commonly used camera parameters. All the renderings have the resolution of 512×512. Following the previous methodologies [32, 33], we evaluate the performance of Era3D on the Google Scanned Object [12] dataset, widely regarded as a standard benchmark for 3D generation tasks. Moreover, we also evaluate our methods on in-the-wild images collected from the Internet or generated by image diffusion models [52] to show the generalization ability. The same as previous methods [55, 69], we remove backgrounds and center objects on these in-the-wild images.

Metrics. Our methodology is evaluated in two tasks, novel view synthesis (NVS) and 3D reconstruction. The NVS quality is evaluated by the Learned Perceptual Image Patch Similarity (LPIPS) [77] between the generated and ground-truth images. LPIPS evaluates the perceptual consistency because there may be slight misalignment between generated and ground-truth images. The 3D reconstruction quality is evaluated by the Chamfer Distance (CD) and the Volume IOU between the reconstructed meshes and the ground truth ones.

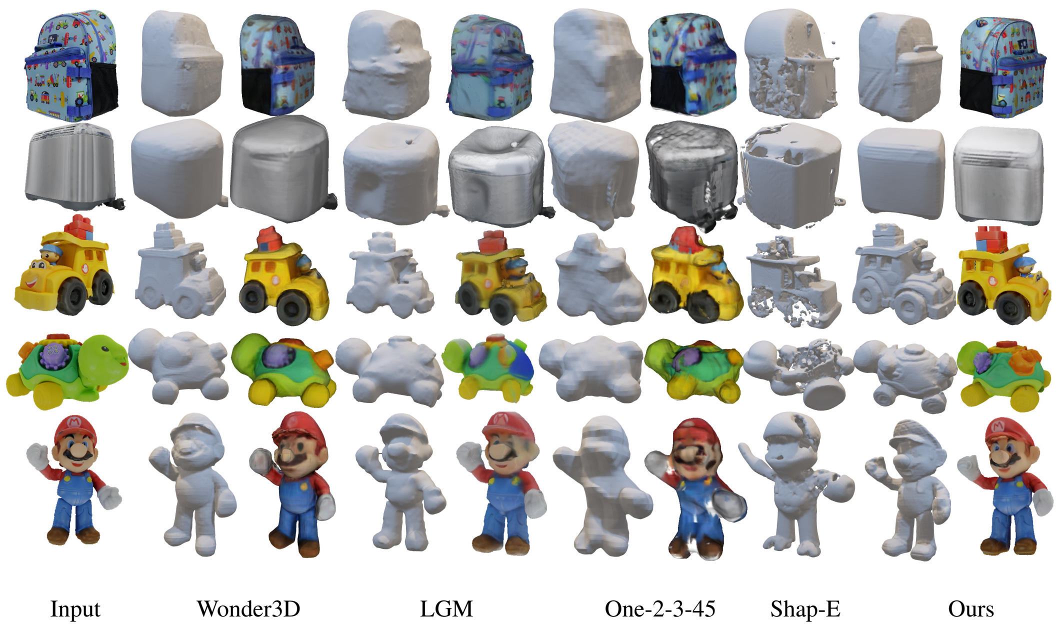

Figure 5: Qualitative comparison of 3D reconstruction results on the GSO dataset [12]. Era3D produces the most high-quality 3D meshes with more details than baseline methods.

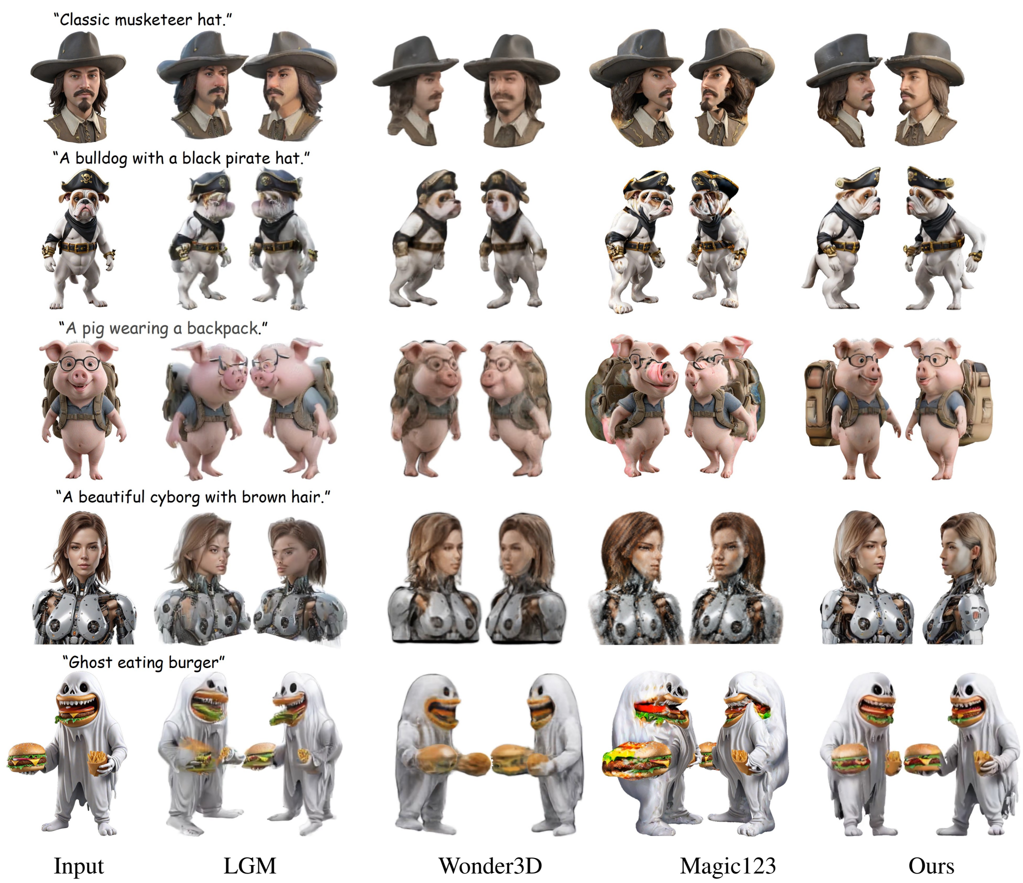

Figure 6: Qualitative comparisons of novel view synthesis quality of reconstructed 3D meshes with single-view images generated by SDXL [45].

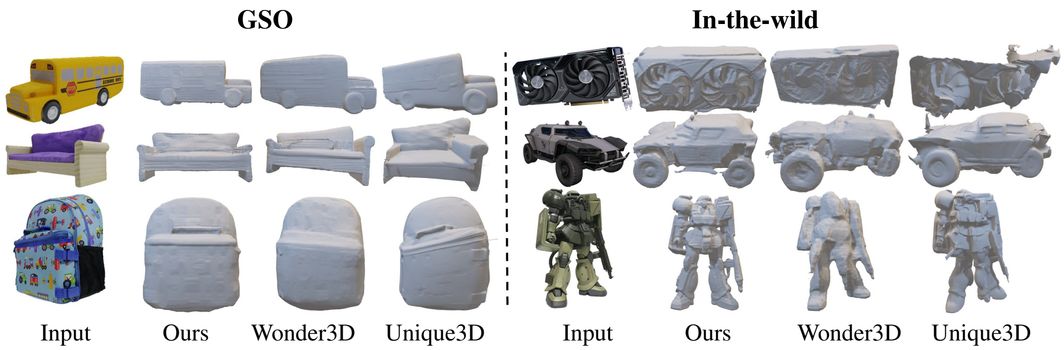

Figure 7: More comparisons w.r.t distortion problem.

Implementation details. Our implementation is built upon the open-source text-to-image model, SD2.1-unclip [51]. We train Era3D on 16 H800 GPUs (each with 80 GB) using a batch size of 128 for 40,000 steps. We set the initial learning rate as 1e-4 and decreased it to 5e-5 after 5,000 steps. The training process takes approximately 30 hours. To conduct classifier-free guidance (CFG) [18], we randomly omit the clip condition at a rate of 0.05. During inference, we employ the DDIM sampler [57] with 40 steps and a CFG scale of 3.0 for the generation. Following Wonder3D [34], we first perform reconstruction with NeuS and then apply a texture refinement step. The whole pipeline requires approximately 4 minutes, comprising 13 seconds for the multiview diffusion, 3 minutes for the NeuS reconstruction, and 10 seconds for the texture refinement. For further details, please refer to the supplementary material.

4.1 Experimental Results

Novel view synthesis. First, several examples of the multiview images and normal maps generated by Era3D are shown in Fig. 1. The results demonstrate that given input images with varying focal lengths and viewpoints, Era3D can generate high-quality and consistent multiview images and normal maps. When the input image is captured by a perspective camera and its viewpoint is not on an elevation of $0°$, Era3D can correctly perceive the elevation of the viewpoint and the perspective distortion. Then, our method learns to generate images of the same object with high fidelity using orthogonal cameras on canonical viewpoints, effectively reducing the artifacts caused by the perspective distortion and improving the reconstruction quality. Moreover, Era3D can produce images in the 512×512 resolution, which enables generating much more details like the fine-grained texture on the "Armor" and the complex structures on the "Mecha" in Fig. 1.

Furthermore, we provide a quantitative comparison with other single-view reconstruction methods including RealFusion [35], Zero-1-to-3 [32], SyncDreamer [33] and Wonder3D [34] in Tab. 1. The results show that our method outperforms previous approaches in terms of novel-view-synthesis quality by a significant margin, showcasing the effectiveness of our designs.

Reconstruction. We further conduct experiments to evaluate the quality of reconstructed 3D meshes. We compare our method with RealFusion [35], Zero-1-to-3 [32], One-2-3-45 [31], Shap-E [21], Magic123[49], Wonder3D [34], SyncDreamer [33], and LGM [61]. Reconstructed meshes and their textures on the GSO dataset are shown in Fig. 5 while the renderings of the reconstructed meshes on text-generated images are shown in Fig. 6. As shown in the results, Shap-E fails to generate completed structures. The meshes reconstructed by One-2-3-45 and LGM tend to be over-smoothed and lack details due to the multiview inconsistency in generated images by Zero-1-to-3 [32] or ImageDream [69]. The results of Wonder3D tend to be distorted on these input images rendered with a focal length of 35mm because it assumes the input images are captured by orthogonal cameras. In contrast, our results show significant improvements in terms of completeness and details than these baseline methods.

Quantitative comparisons of Chamfer Distance (CD) and Intersection over Union (IoU) are shown in Tab. 1. Era3D outperforms all other methods, exhibiting lower Chamfer Distance and higher Volume IoU, suggesting that the meshes it generates align more closely with the actual 3D models.

Distortion problem We finally provide the comparisons with SOTA methods, like Unique3D, w.r.t distortion problem in Fig. 7, which shows that they suffers from severe perspective distortion while our method greatly alleviates this problem.

Table 1: Quantitative evaluation of Chamfer distance, IoU (for reconstruction), and LPIPS (for NVS).

Method	CD ↓	IoU↑	LPIPS ↓	SSIM ↑	PSNR ↑
RealFusion	0.0819	0.2714	0.283	0.722	15.26
Zero-1-to-3	0.0339	0.5035	0.166	0.779	18.93
One-2-3-45	0.0629	0.4086	-	-	-
Shap-E	0.0436	0.3584	-	-	-
Magic123	0.0516	0.4528	-	-	-
SyncDreamer	0.0261	0.5421	0.146	0.798	20.05
Wonder3D	0.0248	0.5678	0.141	0.811	20.83
LGM	0.0259	0.5628	-	-	-
Ours	**0.0217**	**0.5973**	**0.126**	**0.837**	**22.74**

Table 2: Comparison of pose estimation accuracy. $\tilde{\alpha}$: elevation, $\tilde{f}$: normlized focal length.

Method		$\tilde{\alpha}$ / °	$\tilde{f}$ / mm
Error	Dino	10.24	0.28
	One-2-3-45	10.14	-
	Ours	**2.69**	**0.13**
Variance	Dino	377.07	0.058
	One-2-3-45	267.44	-
	Ours	**112.30**	**0.036**

4.2 Accuracy of Estimated Elevations and Focal Lengths

Beyond the tasks already discussed, we further evaluate the pose prediction of Era3D on the GSO dataset. We render the images with an elevation of $[-10, 40]$ degrees and focal lengths of $\{35, 50, 85, 105, 135, \infty\}$, respectively. As a baseline method, we employ dinov2_vitb14 feature [40] to predict the pose and train it with the same dataset. We compare our predictions with this baseline method and One-2-3-45. As shown in Tab. 2, Era3D achieves superior performance in error and variance. A more detailed analysis is provided in the supplementary materials.

4.3 Ablations and Discussions

Regression and condition scheme. In Fig. 8, we remove the EFReg and compare the results with our full model to demonstrate the effectiveness of our design. Without regressing a focal length and elevation as conditions during the denoising process, the resulting shape is distorted and fails to generate reasonable novel views in the canonical camera setting. In comparison, adding our EFReg module and conditioning on the predicted elevations and focal lengths provides effective guidance to generate undistorted cross-domain images, thereby resulting in more accurate 3D reconstructions.

Figure 8: Ablation study of EFReg.

Row-wise multiview attention. As illustrated in Fig. 1, our proposed RMA effectively facilitates information exchange among multiview images, yielding consistent results comparable to those achieved by dense multiview attention layers in [69, 34]. In a N-view camera system, assuming a latent feature with size of $S \times S$, our RMA design significantly improves training efficiency by reducing the computational complexity of attention layers from $O(N^2S^4)$ to $O(N^2S^3)$, as shown in Fig. 3. While epipolar attention also achieves a complexity reduction to $O(N^2S^2K)$, where K is the sample number, it does so at the cost of increased memory and time consumption due to the sampling process. To further highlight the efficiency of RMA over dense multiview attention, we present the memory usage and running time of both 256 and 512 resolutions. We use the epipolar attention implementation in [22]. As listed in Tab. 3, the advantage of RMA becomes increasingly obvious as the resolution grows. At a resolution of 512, RMA achieves a thirty-fold reduction in memory usage and a nearly hundred-fold reduction in running time. Even with xFormers [26], our method substantially improves training efficiency by a large margin (22.9 ms vs. 1.86 ms). This efficiency enables training models on higher resolutions or with denser views without significantly increasing computational efficiency and demand, thereby maintaining a lightweight framework.

Finally, we conduct performance comparisons between dense, epipolar, and our row-wise attention. Considering that in our orthogonal setup with the same elevation, epipolar attention is equivalent to row-wise attention (except for implementation differences), we compared dense and row-wise attention at a resolution of 256. Era3D achieves comparable performance with dense multiview attention, as evidenced in Tab. 4. Our row-wise setting outperforms the baseline for the Chamfer

Table 3: Memory usage and running time of multiview attention with resolution of 256 and 512.

Multiview attention	w/o xFormers				w/ xFormers			
	Memory usage (G)		Running time (ms)		Memory usage (G)		Running time (ms)	
	256	512	256	512	256	512	256	512
Dense	3.02	35.32	8.88	220.41	**0.99**	1.42	1.77	22.96
Epipolar	2.43	24.20	3.57	60.89	1.02	1.71	1.78	20.03
Row-wise	**0.95**	**1.66**	**0.91**	**2.23**	**0.99**	**1.08**	**0.28**	**1.86**

Table 4: Performance of dense and row-wise attention at a resolution of 256.

Method	CD ↓	IoU ↑	LPIPS ↓	PSNR ↑	SSIM ↑
dense	0.0239	0.5877	0.140	20.73	0.819
rowwise	0.0232	0.5831	0.137	20.92	0.813

distance, LPIPS, and PSNR. We attribute this to row-wise attention reducing the number of attention tokens, allowing the model to focus more on valuable tokens.

5 Limitation and Conclusion

Limitations. Though Era3D achieves improvements on the multiview generation task, our method struggles to generate intricate geometries like thin structures because we only generate 6 multiview images and such sparse generated images have difficulty in modeling complex geometries. Since the reconstruction algorithm is based on Neural SDF, Era3D cannot reconstruct meshes with open surfaces. In future works, we could integrate our framework with other 3D representations, such as Gaussian splatting, to improve both rendering and geometry quality.

Conclusion. In this paper, we present Era3D, a high-quality multiview generation method for single-view 3D reconstruction. In Era3D, we propose to generate images in a canonical camera setting while allowing input images to have arbitrary camera intrinsics and viewpoints. To improve the generation quality, we design a regression and condition scheme to predict the focal length and elevation of input images, which are further conditioned to the diffusion process. Additionally, we employ row-wise multiview attention to replace dense attention, significantly reducing computational workloads and facilitating high-resolution cross-view generation. Compared with baseline methods, Era3D achieves superior geometry quality in single-view 3D reconstruction.

6 Ethics Statement

The objective of Era3D is to equip users with a powerful tool for creating detailed 3D models. Our method allows users to generate 3D objects based on a single image. However, there is a potential risk that these generated models could be misused to deceive viewers. It is important to note that this issue is not unique to our methodology but prevalent in other generative model methodologies. Therefore, it is absolutely essential for current and future research in the field of 3D generative modeling to address and reassess these considerations consistently.

Acknowledgments and Disclosure of Funding

The research was supported by Theme-based Research Scheme (T45-205/21-N) from Hong Kong RGC, and Generative AI Research and Development Centre from InnoHK.

References

[1] Jonathan T Barron, Ben Mildenhall, Dor Verbin, Pratul P Srinivasan, and Peter Hedman. Mip-nerf 360: Unbounded anti-aliased neural radiance fields. In Proceedings of the IEEE/CVF Conference on Computer Vision and Pattern Recognition, pages 5470–5479, 2022.

[2] Andreas Blattmann, Tim Dockhorn, Sumith Kulal, Daniel Mendelevitch, Maciej Kilian, Dominik Lorenz, Yam Levi, Zion English, Vikram Voleti, Adam Letts, et al. Stable video diffusion: Scaling latent video diffusion models to large datasets. arXiv preprint arXiv:2311.15127, 2023.

[3] Eric R Chan, Connor Z Lin, Matthew A Chan, Koki Nagano, Boxiao Pan, Shalini De Mello, Orazio Gallo, Leonidas J Guibas, Jonathan Tremblay, Sameh Khamis, et al. Efficient geometry-aware 3d generative adversarial networks. In Proceedings of the IEEE/CVF conference on computer vision and pattern recognition, pages 16123–16133, 2022.

[4] Angel X Chang, Thomas Funkhouser, Leonidas Guibas, Pat Hanrahan, Qixing Huang, Zimo Li, Silvio Savarese, Manolis Savva, Shuran Song, Hao Su, et al. Shapenet: An information-rich 3d model repository. arXiv preprint arXiv:1512.03012, 2015.

[5] David Charatan, Sizhe Li, Andrea Tagliasacchi, and Vincent Sitzmann. pixelsplat: 3d gaussian splats from image pairs for scalable generalizable 3d reconstruction. arXiv preprint arXiv:2312.12337, 2023.

[6] Rui Chen, Yongwei Chen, Ningxin Jiao, and Kui Jia. Fantasia3d: Disentangling geometry and appearance for high-quality text-to-3d content creation. In Proceedings of the IEEE/CVF International Conference on Computer Vision, pages 22246–22256, 2023.

[7] Ting Chen. On the importance of noise scheduling for diffusion models. arXiv preprint arXiv:2301.10972, 2023.

[8] Zilong Chen, Yikai Wang, Feng Wang, Zhengyi Wang, and Huaping Liu. V3d: Video diffusion models are effective 3d generators. arXiv preprint arXiv:2403.06738, 2024.

[9] Yen-Chi Cheng, Hsin-Ying Lee, Sergey Tulyakov, Alexander G Schwing, and Liang-Yan Gui. Sdfusion: Multimodal 3d shape completion, reconstruction, and generation. In Proceedings of the IEEE/CVF Conference on Computer Vision and Pattern Recognition, pages 4456–4465, 2023.

[10] Matt Deitke, Dustin Schwenk, Jordi Salvador, Luca Weihs, Oscar Michel, Eli VanderBilt, Ludwig Schmidt, Kiana Ehsani, Aniruddha Kembhavi, and Ali Farhadi. Objaverse: A universe of annotated 3d objects. In Proceedings of the IEEE/CVF Conference on Computer Vision and Pattern Recognition, pages 13142–13153, 2023.

[11] Prafulla Dhariwal and Alexander Nichol. Diffusion models beat gans on image synthesis. Advances in neural information processing systems, 34:8780–8794, 2021.

[12] Laura Downs, Anthony Francis, Nate Koenig, Brandon Kinman, Ryan Hickman, Krista Reymann, Thomas B McHugh, and Vincent Vanhoucke. Google scanned objects: A high-quality dataset of 3d scanned household items. In 2022 International Conference on Robotics and Automation (ICRA), pages 2553–2560. IEEE, 2022.

[13] Ian Goodfellow, Jean Pouget-Abadie, Mehdi Mirza, Bing Xu, David Warde-Farley, Sherjil Ozair, Aaron Courville, and Yoshua Bengio. Generative adversarial nets. In NeurIPS, 2014.

[14] Jiatao Gu, Lingjie Liu, Peng Wang, and Christian Theobalt. Stylenerf: A style-based 3d-aware generator for high-resolution image synthesis. arXiv preprint arXiv:2110.08985, 2021.

[15] Anchit Gupta, Wenhan Xiong, Yixin Nie, Ian Jones, and Barlas Oğuz. 3dgen: Triplane latent diffusion for textured mesh generation. arXiv preprint arXiv:2303.05371, 2023.

[16] Jonathan Ho, Ajay Jain, and Pieter Abbeel. Denoising diffusion probabilistic models. Advances in neural information processing systems, 33:6840–6851, 2020.

[17] Jonathan Ho, Ajay Jain, and Pieter Abbeel. Denoising diffusion probabilistic models. NeurIPS, 2020.

[18] Jonathan Ho and Tim Salimans. Classifier-free diffusion guidance. arXiv preprint arXiv:2207.12598, 2022.

[19] Yicong Hong, Kai Zhang, Jiuxiang Gu, Sai Bi, Yang Zhou, Difan Liu, Feng Liu, Kalyan Sunkavalli, Trung Bui, and Hao Tan. Lrm: Large reconstruction model for single image to 3d. arXiv preprint arXiv:2311.04400, 2023.

[20] Hanwen Jiang, Zhenyu Jiang, Yue Zhao, and Qixing Huang. Leap: Liberate sparse-view 3d modeling from camera poses. arXiv preprint arXiv:2310.01410, 2023.

[21] Heewoo Jun and Alex Nichol. Shap-e: Generating conditional 3d implicit functions. arXiv preprint arXiv:2305.02463, 2023.

[22] Yash Kant, Ziyi Wu, Michael Vasilkovsky, Guocheng Qian, Jian Ren, Riza Alp Guler, Bernard Ghanem, Sergey Tulyakov, Igor Gilitschenski, and Aliaksandr Siarohin. Spad: Spatially aware multiview diffusers. arXiv preprint arXiv:2402.05235, 2024.

[23] Tero Karras, Samuli Laine, and Timo Aila. A style-based generator architecture for generative adversarial networks. In CVPR, 2019.

[24] Bernhard Kerbl, Georgios Kopanas, Thomas Leimkühler, and George Drettakis. 3d gaussian splatting for real-time radiance field rendering. ACM Transactions on Graphics, 42(4):1–14, 2023.

[25] Samuli Laine, Janne Hellsten, Tero Karras, Yeongho Seol, Jaakko Lehtinen, and Timo Aila. Modular primitives for high-performance differentiable rendering. ACM Transactions on Graphics, 39(6), 2020.

[26] Benjamin Lefaudeux, Francisco Massa, Diana Liskovich, Wenhan Xiong, Vittorio Caggiano, Sean Naren, Min Xu, Jieru Hu, Marta Tintore, Susan Zhang, Patrick Labatut, Daniel Haziza, Luca Wehrstedt, Jeremy Reizenstein, and Grigory Sizov. xformers: A modular and hackable transformer modelling library. `https://github.com/facebookresearch/xformers`, 2022.

[27] Jiahao Li, Hao Tan, Kai Zhang, Zexiang Xu, Fujun Luan, Yinghao Xu, Yicong Hong, Kalyan Sunkavalli, Greg Shakhnarovich, and Sai Bi. Instant3d: Fast text-to-3d with sparse-view generation and large reconstruction model. arXiv preprint arXiv:2311.06214, 2023.

[28] Peng Li, Jiayin Zhao, Jingyao Wu, Chao Deng, Yuqi Han, Haoqian Wang, and Tao Yu. Opal: Occlusion pattern aware loss for unsupervised light field disparity estimation. IEEE Transactions on Pattern Analysis and Machine Intelligence, 2023.

[29] Chen-Hsuan Lin, Jun Gao, Luming Tang, Towaki Takikawa, Xiaohui Zeng, Xun Huang, Karsten Kreis, Sanja Fidler, Ming-Yu Liu, and Tsung-Yi Lin. Magic3d: High-resolution text-to-3d content creation. In Proceedings of the IEEE/CVF Conference on Computer Vision and Pattern Recognition, pages 300–309, 2023.

[30] Minghua Liu, Chao Xu, Haian Jin, Linghao Chen, Mukund Varma T, Zexiang Xu, and Hao Su. One-2-3-45: Any single image to 3d mesh in 45 seconds without per-shape optimization. Advances in Neural Information Processing Systems, 36, 2024.

[31] Minghua Liu, Chao Xu, Haian Jin, Linghao Chen, Zexiang Xu, Hao Su, et al. One-2-3-45: Any single image to 3d mesh in 45 seconds without per-shape optimization. arXiv preprint arXiv:2306.16928, 2023.

[32] Ruoshi Liu, Rundi Wu, Basile Van Hoorick, Pavel Tokmakov, Sergey Zakharov, and Carl Vondrick. Zero-1-to-3: Zero-shot one image to 3d object. In Proceedings of the IEEE/CVF International Conference on Computer Vision, pages 9298–9309, 2023.

[33] Yuan Liu, Cheng Lin, Zijiao Zeng, Xiaoxiao Long, Lingjie Liu, Taku Komura, and Wenping Wang. Syncdreamer: Generating multiview-consistent images from a single-view image. arXiv preprint arXiv:2309.03453, 2023.

[34] Xiaoxiao Long, Yuan-Chen Guo, Cheng Lin, Yuan Liu, Zhiyang Dou, Lingjie Liu, Yuexin Ma, Song-Hai Zhang, Marc Habermann, Christian Theobalt, et al. Wonder3d: Single image to 3d using cross-domain diffusion. arXiv preprint arXiv:2310.15008, 2023.

[35] Luke Melas-Kyriazi, Christian Rupprecht, Iro Laina, and Andrea Vedaldi. Realfusion: 360° reconstruction of any object from a single image. In Arxiv, 2023.

[36] Ben Mildenhall, Pratul P Srinivasan, Matthew Tancik, Jonathan T Barron, Ravi Ramamoorthi, and Ren Ng. Nerf: Representing scenes as neural radiance fields for view synthesis. Communications of the ACM, 65(1):99–106, 2021.

[37] Thomas Müller, Alex Evans, Christoph Schied, and Alexander Keller. Instant neural graphics primitives with a multiresolution hash encoding. ACM transactions on graphics (TOG), 41(4):1–15, 2022.

[38] Michael Niemeyer and Andreas Geiger. Giraffe: Representing scenes as compositional generative neural feature fields. In CVPR, 2021.

[39] Matthias Nießner, Michael Zollhöfer, Shahram Izadi, and Marc Stamminger. Real-time 3d reconstruction at scale using voxel hashing. ACM Transactions on Graphics (ToG), 32(6):1–11, 2013.

[40] Maxime Oquab, Timothée Darcet, Theo Moutakanni, Huy V. Vo, Marc Szafraniec, Vasil Khalidov, Pierre Fernandez, Daniel Haziza, Francisco Massa, Alaaeldin El-Nouby, Russell Howes, Po-Yao Huang, Hu Xu, Vasu Sharma, Shang-Wen Li, Wojciech Galuba, Mike Rabbat, Mido Assran, Nicolas Ballas, Gabriel Synnaeve, Ishan Misra, Herve Jegou, Julien Mairal, Patrick Labatut, Armand Joulin, and Piotr Bojanowski. Dinov2: Learning robust visual features without supervision, 2023.

[41] Roy Or-El, Xuan Luo, Mengyi Shan, Eli Shechtman, Jeong Joon Park, and Ira Kemelmacher-Shlizerman. Stylesdf: High-resolution 3d-consistent image and geometry generation. In CVPR, 2022.

[42] Jeong Joon Park, Peter Florence, Julian Straub, Richard Newcombe, and Steven Lovegrove. Deepsdf: Learning continuous signed distance functions for shape representation. In Proceedings of the IEEE/CVF conference on computer vision and pattern recognition, pages 165–174, 2019.

[43] Jeong Joon Park, Peter Florence, Julian Straub, Richard Newcombe, and Steven Lovegrove. Deepsdf: Learning continuous signed distance functions for shape representation. In CVPR, 2019.

[44] Songyou Peng, Michael Niemeyer, Lars Mescheder, Marc Pollefeys, and Andreas Geiger. Convolutional occupancy networks. In Computer Vision–ECCV 2020: 16th European Conference, Glasgow, UK, August 23–28, 2020, Proceedings, Part III 16, pages 523–540. Springer, 2020.

[45] Dustin Podell, Zion English, Kyle Lacey, Andreas Blattmann, Tim Dockhorn, Jonas Müller, Joe Penna, and Robin Rombach. Sdxl: Improving latent diffusion models for high-resolution image synthesis. arXiv preprint arXiv:2307.01952, 2023.

[46] Ben Poole, Ajay Jain, Jonathan T Barron, and Ben Mildenhall. Dreamfusion: Text-to-3d using 2d diffusion. arXiv preprint arXiv:2209.14988, 2022.

[47] Xingqun Qi, Jiahao Pan, Peng Li, Ruibin Yuan, Xiaowei Chi, Mengfei Li, Wenhan Luo, Wei Xue, Shanghang Zhang, Qifeng Liu, et al. Weakly-supervised emotion transition learning for diverse 3d co-speech gesture generation. In Proceedings of the IEEE/CVF Conference on Computer Vision and Pattern Recognition, pages 10424–10434, 2024.

[48] Xingqun Qi, Hengyuan Zhang, Yatian Wang, Jiahao Pan, Chen Liu, Peng Li, Xiaowei Chi, Mengfei Li, Qixun Zhang, Wei Xue, et al. Cocogesture: Toward coherent co-speech 3d gesture generation in the wild. arXiv preprint arXiv:2405.16874, 2024.

[49] Guocheng Qian, Jinjie Mai, Abdullah Hamdi, Jian Ren, Aliaksandr Siarohin, Bing Li, Hsin-Ying Lee, Ivan Skorokhodov, Peter Wonka, Sergey Tulyakov, et al. Magic123: One image to high-quality 3d object generation using both 2d and 3d diffusion priors. arXiv preprint arXiv:2306.17843, 2023.

[50] Robin Rombach, Andreas Blattmann, Dominik Lorenz, Patrick Esser, and Björn Ommer. High-resolution image synthesis with latent diffusion models. In CVPR, 2022.

[51] Robin Rombach, Andreas Blattmann, Dominik Lorenz, Patrick Esser, and Björn Ommer. High-resolution image synthesis with latent diffusion models. In Proceedings of the IEEE/CVF Conference on Computer Vision and Pattern Recognition (CVPR), pages 10684–10695, June 2022.

[52] Robin Rombach, Andreas Blattmann, Dominik Lorenz, Patrick Esser, and Björn Ommer. High-resolution image synthesis with latent diffusion models, 2021.

[53] Shunsuke Saito, Zeng Huang, Ryota Natsume, Shigeo Morishima, Angjoo Kanazawa, and Hao Li. Pifu: Pixel-aligned implicit function for high-resolution clothed human digitization. In Proceedings of the IEEE/CVF international conference on computer vision, pages 2304–2314, 2019.

[54] Ruoxi Shi, Hansheng Chen, Zhuoyang Zhang, Minghua Liu, Chao Xu, Xinyue Wei, Linghao Chen, Chong Zeng, and Hao Su. Zero123++: a single image to consistent multi-view diffusion base model. arXiv preprint arXiv:2310.15110, 2023.

[55] Yichun Shi, Peng Wang, Jianglong Ye, Mai Long, Kejie Li, and Xiao Yang. Mvdream: Multi-view diffusion for 3d generation. arXiv preprint arXiv:2308.16512, 2023.

[56] J. Ryan Shue, Eric Ryan Chan, Ryan Po, Zachary Ankner, Jiajun Wu, and Gordon Wetzstein. 3d neural field generation using triplane diffusion. In CVPR, 2023.

[57] Jiaming Song, Chenlin Meng, and Stefano Ermon. Denoising diffusion implicit models. arXiv preprint arXiv:2010.02502, 2020.

[58] Cheng Sun, Min Sun, and Hwann-Tzong Chen. Direct voxel grid optimization: Super-fast convergence for radiance fields reconstruction. In Proceedings of the IEEE/CVF Conference on Computer Vision and Pattern Recognition, pages 5459–5469, 2022.

[59] Stanislaw Szymanowicz, Christian Rupprecht, and Andrea Vedaldi. Splatter image: Ultra-fast single-view 3d reconstruction. arXiv preprint arXiv:2312.13150, 2023.

[60] Stanislaw Szymanowicz, Christian Rupprecht, and Andrea Vedaldi. Viewset diffusion:(0-) image-conditioned 3d generative models from 2d data. In Proceedings of the IEEE/CVF International Conference on Computer Vision, pages 8863–8873, 2023.

[61] Jiaxiang Tang, Zhaoxi Chen, Xiaokang Chen, Tengfei Wang, Gang Zeng, and Ziwei Liu. Lgm: Large multi-view gaussian model for high-resolution 3d content creation. arXiv preprint arXiv:2402.05054, 2024.

[62] Jiaxiang Tang, Jiawei Ren, Hang Zhou, Ziwei Liu, and Gang Zeng. Dreamgaussian: Generative gaussian splatting for efficient 3d content creation. arXiv preprint arXiv:2309.16653, 2023.

[63] Shitao Tang, Jiacheng Chen, Dilin Wang, Chengzhou Tang, Fuyang Zhang, Yuchen Fan, Vikas Chandra, Yasutaka Furukawa, and Rakesh Ranjan. Mvdiffusion++: A dense high-resolution multi-view diffusion model for single or sparse-view 3d object reconstruction. arXiv preprint arXiv:2402.12712, 2024.

[64] Shitao Tang, Fuayng Zhang, Jiacheng Chen, Peng Wang, and Furukawa Yasutaka. Mvdiffusion: Enabling holistic multi-view image generation with correspondence-aware diffusion. arXiv preprint 2307.01097, 2023.

[65] Hung-Yu Tseng, Qinbo Li, Changil Kim, Suhib Alsisan, Jia-Bin Huang, and Johannes Kopf. Consistent view synthesis with pose-guided diffusion models. In Proceedings of the IEEE/CVF Conference on Computer Vision and Pattern Recognition, pages 16773–16783, 2023.

[66] Vikram Voleti, Chun-Han Yao, Mark Boss, Adam Letts, David Pankratz, Dmitry Tochilkin, Christian Laforte, Robin Rombach, and Varun Jampani. Sv3d: Novel multi-view synthesis and 3d generation from a single image using latent video diffusion. arXiv preprint arXiv:2403.12008, 2024.

[67] Haochen Wang, Xiaodan Du, Jiahao Li, Raymond A Yeh, and Greg Shakhnarovich. Score jacobian chaining: Lifting pretrained 2d diffusion models for 3d generation. In Proceedings of the IEEE/CVF Conference on Computer Vision and Pattern Recognition, pages 12619–12629, 2023.

[68] Peng Wang, Lingjie Liu, Yuan Liu, Christian Theobalt, Taku Komura, and Wenping Wang. Neus: Learning neural implicit surfaces by volume rendering for multi-view reconstruction. arXiv preprint arXiv:2106.10689, 2021.

[69] Peng Wang and Yichun Shi. Imagedream: Image-prompt multi-view diffusion for 3d generation. arXiv preprint arXiv:2312.02201, 2023.

[70] Peng Wang, Hao Tan, Sai Bi, Yinghao Xu, Fujun Luan, Kalyan Sunkavalli, Wenping Wang, Zexiang Xu, and Kai Zhang. Pf-lrm: Pose-free large reconstruction model for joint pose and shape prediction. arXiv preprint arXiv:2311.12024, 2023.

[71] Zhengyi Wang, Cheng Lu, Yikai Wang, Fan Bao, Chongxuan Li, Hang Su, and Jun Zhu. Prolificdreamer: High-fidelity and diverse text-to-3d generation with variational score distillation. Advances in Neural Information Processing Systems, 36, 2024.

[72] Zhengyi Wang, Yikai Wang, Yifei Chen, Chendong Xiang, Shuo Chen, Dajiang Yu, Chongxuan Li, Hang Su, and Jun Zhu. Crm: Single image to 3d textured mesh with convolutional reconstruction model. arXiv preprint arXiv:2403.05034, 2024.

[73] Xinyue Wei, Kai Zhang, Sai Bi, Hao Tan, Fujun Luan, Valentin Deschaintre, Kalyan Sunkavalli, Hao Su, and Zexiang Xu. Meshlrm: Large reconstruction model for high-quality mesh. arXiv preprint arXiv:2404.12385, 2024.

[74] Jiale Xu, Weihao Cheng, Yiming Gao, Xintao Wang, Shenghua Gao, and Ying Shan. Instantmesh: Efficient 3d mesh generation from a single image with sparse-view large reconstruction models. arXiv preprint arXiv:2404.07191, 2024.

[75] Yinghao Xu, Zifan Shi, Wang Yifan, Hansheng Chen, Ceyuan Yang, Sida Peng, Yujun Shen, and Gordon Wetzstein. Grm: Large gaussian reconstruction model for efficient 3d reconstruction and generation. arXiv preprint arXiv:2403.14621, 2024.

[76] Yinghao Xu, Hao Tan, Fujun Luan, Sai Bi, Peng Wang, Jiahao Li, Zifan Shi, Kalyan Sunkavalli, Gordon Wetzstein, Zexiang Xu, et al. Dmv3d: Denoising multi-view diffusion using 3d large reconstruction model. arXiv preprint arXiv:2311.09217, 2023.

[77] Richard Zhang, Phillip Isola, Alexei A Efros, Eli Shechtman, and Oliver Wang. The unreasonable effectiveness of deep features as a perceptual metric. In Proceedings of the IEEE conference on computer vision and pattern recognition, pages 586–595, 2018.

[78] Ruichen Zheng, Peng Li, Haoqian Wang, and Tao Yu. Learning visibility field for detailed 3d human reconstruction and relighting. In Proceedings of the IEEE/CVF Conference on Computer Vision and Pattern Recognition, pages 216–226, 2023.

[79] Zi-Xin Zou, Zhipeng Yu, Yuan-Chen Guo, Yangguang Li, Ding Liang, Yan-Pei Cao, and Song-Hai Zhang. Triplane meets gaussian splatting: Fast and generalizable single-view 3d reconstruction with transformers. arXiv preprint arXiv:2312.09147, 2023.

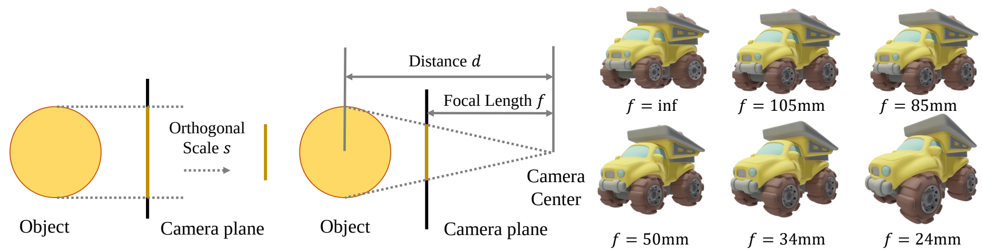

(a) Orthogonal Camera (b) Perspective Camera (c) Renderings with different focal lengths

Figure 9: Equivalence between orthogonal and perspective camera models and our rendering samples in GSO dataset [12].

A Supplementary Material

A.1 Implementation Details

Data preparation. To render training data, we randomly choose a focal length for the input image from a predefined set of focal lengths and we always use the same orthogonal camera for all generated images. To train Era3D, we need to construct an orthogonal camera to render generation images and the equivalent perspective cameras to render input images. The equivalence here means that the renderings from these two kinds of cameras have almost the same size, for reducing training bias. As shown in Fig. 9 (a) and (b), given a predefined orthogonal scale s and a given focal length f, we compute the distance d by $d = f/s$, where s is the orthogonal scale to scale the size of the rendered image. We will adjust the distance from the camera center to the object to the value d to make the rendered image as similar as possible.

Normalized focal length. In our experiment, we choose several discrete focal lengths, $\{24, 35, 50, 85, 105, 135\}$ mm, and an orthogonal camera to render multiview images for training. Due to the broad range of focal lengths, we regress the normalized focal lengths instead of the actual ones. Specifically, we normalize them with minimum focal,

$$\tilde{f} = 24/f. \tag{3}$$

For the orthogonal views, we set $\tilde{f} = 0$.

Cross-domain attention. In contrast to Wonder3D [34], we do not incorporate an additional attention layer to fuse information between cross-domain images. Instead, in earlier experiments, we combined both the cross-domain fusion module and the multiview fusion module within the same row-wise attention block to enhance training efficiency. This initial setup, however, leads to suboptimal outcomes, as shown in Fig. 5, where it tends to produce overly smoothed normal maps. We hypothesize that the significant differences between domain images are the primary cause of this issue, as the row-wise information alone is insufficient for learning fine-grained features across domains. In contrast, integrating the cross-domain module within the self-attention block enables the utilization of complete image features, allowing the model to better handle these disparities and achieve improved generalization. Our attention block consists of self-cross-domain attention, row-wise multiview attention, and cross-domain attention, which allows us to merge the two-stage training into a single-stage joint training, effectively aligning images of both domains.

Table 5: Ablation study on the position of the cross domain-block.

Reconstruction and texture refinement. We perform reconstruction from the generated multiview normal and color images using NeuS. However, since we only generate sparse views, the rendered images of the reconstructed meshes may not attain the quality of the generated ones, particularly for objects with complex textures. To address this issue, we employ differential rendering to refine the textures on the reconstructed meshes. Specifically, we preserve the geometry of Neus and initialize the texture with vertex colors. We utilize [25] to render multiview images in predefined views and optimize the vertex colors with the corresponding generated images. This process takes less than 1 second and significantly improves the texture quality. For the NeuS reconstruction, we use the same settings as Wonder3D. During texture refinement, we optimize the appearance for 200 iterations with a resolution of 1024 and a learning rate of 1e-3.

Noise scheduler. The original SD2.1-Unclip base model employs a scaled linear noise scheduler during training, which is effective for smaller sample sizes, such as 256. However, this scheduler tends to restrict the generative capabilities of models at larger sizes, such as 512. Drawing inspiration from recent research by Chen [7], we implemented a linear noise scheduler throughout our experiments to enhance generation quality and accelerate the convergence of the background. This adjustment proves critical in supporting the model's performance and efficiency.

A.2 Proof of Proposition 1

Given two cameras O_1 and O_2 with relative rotation R and translation t, let x_1 and x_2 denote the homogeneous coordinates of corresponding points in the image planes, respectively, epipolar constraint can be expressed as

$$x_2^T E x_1 = 0, \tag{4}$$

where E is the fundamental matrix. Then, the epipolar line in O_2 can be represented as

$$l = Ex_1, E = [t]_\times R, \tag{5}$$

where $[t]_\times$ denotes the skew-symmetric matrix generated by t. However, epipolar attention needs to query dense points on epipolar lines, which leads to significant computational inefficiency, due to arbitrary directions and varying lengths of epipolar lines.

Row-wise multiview attention is a special epipolar attention in our defined canonical camera setting, as depicted in Fig. 3(d). Assuming the y-axis represents the gravity direction, the x-axis denotes the right-hand direction, and the z-axis points away from the camera to the origin of the object. The relative R and t between two cameras can be represented as

$$R = \begin{bmatrix} cos(\theta) & 0 & sin(\theta) \\ 0 & 1 & 0 \\ -sin(\theta) & 0 & cos(\theta) \end{bmatrix}, t = [t_x, 0, t_z]^T, \tag{6}$$

where θ is the azimuth angle of the cameras. Considering the point $P_1(x_1, y_1, z_1)$ in camera $O_1^{'}$, the coordinates of P_1 in camera $O_2^{'}$ are given by

$$P_2(x_2, y_2, z_2) = RP_1 + t = \begin{bmatrix} cos(\theta)x + sin(\theta)z_1 + t_x \\ y_1 \\ cos(\theta)z - sin(\theta)x_1 + t_z \end{bmatrix}. \tag{7}$$

It is observed that the scene points from different views share the same y-coordinate. Assuming the identical orthographic scale, the y-coordinates of projections on the image plane are also equivalent. Extending a single sample to a line of points with the same y-coordinate, all projections of those points on two image planes are on the same row.

A.3 Pose Estimation

During inference, we obtain the final pose by averaging the class-free guidance results from all denoising steps,

$$\begin{aligned} \tilde{\alpha} &= \frac{1}{T}\sum_{t=1}^{T}[(1+w)\alpha_\theta^t(z,c) - w\alpha_\theta^t(z)], \\ \tilde{f} &= \frac{1}{T}\sum_{t=1}^{T}[(1+w)f_\theta^t(z,c) - wf_\theta^t(z)], \end{aligned} \tag{8}$$

where z is the latent, c is the condition, w is the CFG scale, θ is the parameters of UNet and MLP and T is the denoising step. We observe that the averaged class-free guidance predictions achieve the highest accuracy. We attribute this to the random dropping of condition images during training. We do not rely solely on the prediction at the final step because we constrain the estimated elevation and focal length with the ground pose rather than the noisy ones at each denoising step. We conduct extensive experiments to evaluate the accuracy of the estimated pose on the GSO dataset.

Elevation. As listed in Tab. 6, Dino and One-2-3-45 only learn the relative trend as the elevation increases, resulting in large errors for cases with high elevations. This is because our baseline only employs the feature of a single image, which is insufficient for predicting the absolute elevation. The prediction of One-2-3-45 mainly depends on the multiview images generated by Zero-1-to-3. The inconsistency of generated images leads to ambiguity in prediction. In comparison, our results are closer to the ground truth elevation. In most cases, the variance of our method is significantly lower than that of Dino and One-2-3-45, demonstrating remarkable robustness.

Focal. We report the error and variance of normalized focal predictions for the baseline and our method in Tab. 7. It is observed that the baseline cannot distinguish the differences between various focal lengths. In contrast, our

Table 6: Elevation accuracy on GSO dataset.

Method		-10 Pred	-10 Err	0 Pred	0 Err	10 Pred	10 Err	20 Pred	20 Err	30 Pred	30 Err	40 Pred	40 Err
Mean	Dino	-13.58	3.58	-6.83	6.83	4.63	5.37	10.21	9,79	16.72	14.28	18.41	21.59
	One-2-3-45	-11.93	1.93	-5.23	5.23	-0.06	10.06	11.17	8.83	15.5	14.5	19.73	20.27
	Ours	-9.71	**0.29**	-2.20	**2.20**	5.59	**4.41**	23.85	**3.85**	34.03	**4.03**	38.67	**1.33**
Var	Dino	202.37	-	252.51	-	**153.67**	-	365.32	-	463.92	-	824.63	-
	One-2-3-45	175.02	-	103.64	-	168.61	-	200.97	-	326.05	-	630.32	-
	Ours	**32.1**	-	**83.63**	-	163.38	-	**113.55**	-	**134.69**	-	**146.46**	-

Table 7: Focal length accuracy on GSO dataset.

Method		0.68 (35) Pred	Err	0.48 (50) Pred	Err	0.28 (85) Pred	Err	0.22 (105) Pred	Err	0.17 (135) Pred	Err	0.0 (ortho) Pred	Err
Mean	Dino	0.75	0.07	0.46	0.02	0.53	0.27	0.56	0.34	0.57	0.4	0.59	0.59
	Ours	0.69	0.01	0.54	0.06	0.37	0.09	0.33	0.11	0.34	0.17	0.32	0.32
var	Dino	0.069	-	0.073	-	0.054	-	0.049	-	0.052	-	0.049	-
	Ours	0.041	-	0.035	-	0.024	-	0.02	-	0.069	-	0.032	-

Normalized focal length (focal length / mm)

Elevation = -10° Elevation = 10° Elevation = 20° Elevation = 0°

Figure 10: Generation results of various elevation. We use reconstructions from the view of Elevation = 0° as the reference. Different inputs generate consistent results.

Focal = 35mm Focal = 85mm Focal = 135mm Ortho

Figure 11: Generation results of various distortions. We employ reconstructions from orthogonal inputs as the reference. For each case, we illustrate the input along with the generated color, normal, and mesh.

Table 8: Quantitative evaluation on images with various focal lengths. CD: Chamfer Distance.

Pose	α=0					f=∞					α=0
	f=35	f=50	f=85	f=105	f=135	α=-10	α=10	α=20	α=30	α=40	$f=\infty$
CD	0.0223	0.0219	0.0216	0.0214	0.0214	0.0217	0.0216	0.216	0.0219	0.0217	0.0213

model can predict the large distortion (e.g., focal=35, 50) of input images, which is advantageous for correcting them to some extent. Simultaneously, our method exhibits smaller errors for settings with large focal lengths than the baseline. We believe our method could be further explored and improved in the future.

Furthermore, we use orthogonal renderings at an elevation of 0 degree as the reference. We vary the elevation from -10 to 40 degrees and select focal lengths from $\{35, 50, 85, 105, 135, \infty\}$ to assess the system's robustness to elevations and focal distortions by reconstructed meshes. As indicated in Tab. 8, the orthogonal setting at elevation 0 achieves the best performance of CD, and other settings are on the same bar with the reference setting, suggesting that our method effectively handles these distortions, producing meshes that align well with the reference ones, even under significant focal distortion. We visualize some samples in Fig. 10 and Fig. 11.

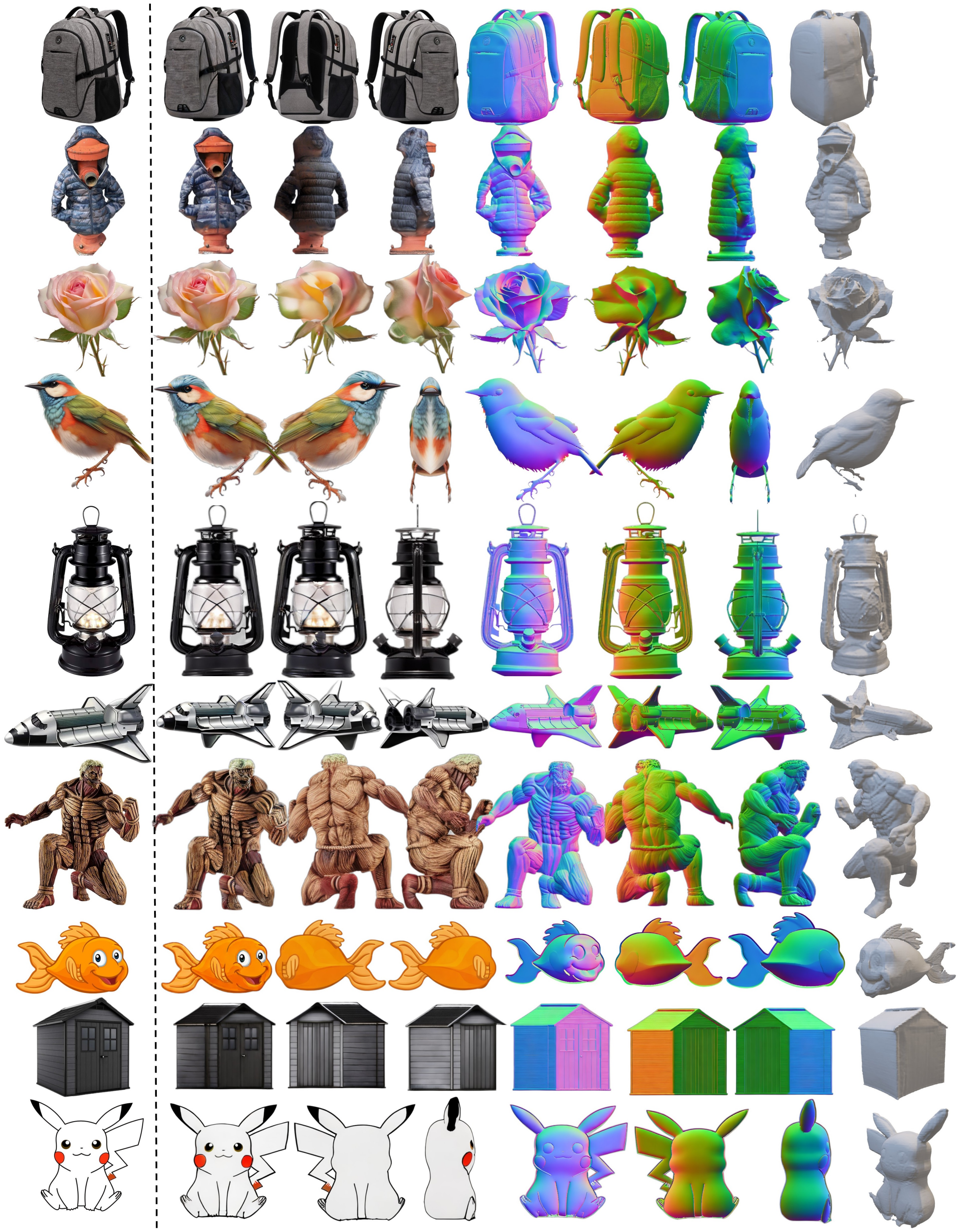

Figure 12: More results of images from the Internet.

NeurIPS Paper Checklist

1. **Claims**

   Question: Do the main claims made in the abstract and introduction accurately reflect the paper's contributions and scope?

   Answer: [Yes]

   Justification: All the claims are supported by the results of experiments.

   Guidelines:

   - The answer NA means that the abstract and introduction do not include the claims made in the paper.
   - The abstract and/or introduction should clearly state the claims made, including the contributions made in the paper and important assumptions and limitations. A No or NA answer to this question will not be perceived well by the reviewers.
   - The claims made should match theoretical and experimental results, and reflect how much the results can be expected to generalize to other settings.
   - It is fine to include aspirational goals as motivation as long as it is clear that these goals are not attained by the paper.

2. **Limitations**

   Question: Does the paper discuss the limitations of the work performed by the authors?

   Answer: [Yes]

   Justification: Our method has difficulty in modeling complex geometries and open meshes.

   Guidelines:

   - The answer NA means that the paper has no limitation while the answer No means that the paper has limitations, but those are not discussed in the paper.
   - The authors are encouraged to create a separate "Limitations" section in their paper.
   - The paper should point out any strong assumptions and how robust the results are to violations of these assumptions (e.g., independence assumptions, noiseless settings, model well-specification, asymptotic approximations only holding locally). The authors should reflect on how these assumptions might be violated in practice and what the implications would be.
   - The authors should reflect on the scope of the claims made, e.g., if the approach was only tested on a few datasets or with a few runs. In general, empirical results often depend on implicit assumptions, which should be articulated.
   - The authors should reflect on the factors that influence the performance of the approach. For example, a facial recognition algorithm may perform poorly when image resolution is low or images are taken in low lighting. Or a speech-to-text system might not be used reliably to provide closed captions for online lectures because it fails to handle technical jargon.
   - The authors should discuss the computational efficiency of the proposed algorithms and how they scale with dataset size.
   - If applicable, the authors should discuss possible limitations of their approach to address problems of privacy and fairness.
   - While the authors might fear that complete honesty about limitations might be used by reviewers as grounds for rejection, a worse outcome might be that reviewers discover limitations that aren't acknowledged in the paper. The authors should use their best judgment and recognize that individual actions in favor of transparency play an important role in developing norms that preserve the integrity of the community. Reviewers will be specifically instructed to not penalize honesty concerning limitations.

3. **Theory Assumptions and Proofs**

   Question: For each theoretical result, does the paper provide the full set of assumptions and a complete (and correct) proof?

   Answer: [NA]

   Justification: This work do not contain theoretical result.

   Guidelines:

   - The answer NA means that the paper does not include theoretical results.
   - All the theorems, formulas, and proofs in the paper should be numbered and cross-referenced.
   - All assumptions should be clearly stated or referenced in the statement of any theorems.

- The proofs can either appear in the main paper or the supplemental material, but if they appear in the supplemental material, the authors are encouraged to provide a short proof sketch to provide intuition.
- Inversely, any informal proof provided in the core of the paper should be complemented by formal proofs provided in appendix or supplemental material.
- Theorems and Lemmas that the proof relies upon should be properly referenced.

4. **Experimental Result Reproducibility**

   Question: Does the paper fully disclose all the information needed to reproduce the main experimental results of the paper to the extent that it affects the main claims and/or conclusions of the paper (regardless of whether the code and data are provided or not)?

   Answer: [Yes]

   Justification: We report the experiment details and we will release related codes.

   Guidelines:

   - The answer NA means that the paper does not include experiments.
   - If the paper includes experiments, a No answer to this question will not be perceived well by the reviewers: Making the paper reproducible is important, regardless of whether the code and data are provided or not.
   - If the contribution is a dataset and/or model, the authors should describe the steps taken to make their results reproducible or verifiable.
   - Depending on the contribution, reproducibility can be accomplished in various ways. For example, if the contribution is a novel architecture, describing the architecture fully might suffice, or if the contribution is a specific model and empirical evaluation, it may be necessary to either make it possible for others to replicate the model with the same dataset, or provide access to the model. In general. releasing code and data is often one good way to accomplish this, but reproducibility can also be provided via detailed instructions for how to replicate the results, access to a hosted model (e.g., in the case of a large language model), releasing of a model checkpoint, or other means that are appropriate to the research performed.
   - While NeurIPS does not require releasing code, the conference does require all submissions to provide some reasonable avenue for reproducibility, which may depend on the nature of the contribution. For example
     (a) If the contribution is primarily a new algorithm, the paper should make it clear how to reproduce that algorithm.
     (b) If the contribution is primarily a new model architecture, the paper should describe the architecture clearly and fully.
     (c) If the contribution is a new model (e.g., a large language model), then there should either be a way to access this model for reproducing the results or a way to reproduce the model (e.g., with an open-source dataset or instructions for how to construct the dataset).
     (d) We recognize that reproducibility may be tricky in some cases, in which case authors are welcome to describe the particular way they provide for reproducibility. In the case of closed-source models, it may be that access to the model is limited in some way (e.g., to registered users), but it should be possible for other researchers to have some path to reproducing or verifying the results.

5. **Open access to data and code**

   Question: Does the paper provide open access to the data and code, with sufficient instructions to faithfully reproduce the main experimental results, as described in supplemental material?

   Answer: [No]

   Justification: Our evaluation uses the public datasets. We do not provide code in Supplementary Material. But they will be made publicly available once they have been fully prepared.

   Guidelines:

   - The answer NA means that paper does not include experiments requiring code.
   - Please see the NeurIPS code and data submission guidelines (`https://nips.cc/public/guides/CodeSubmissionPolicy`) for more details.
   - While we encourage the release of code and data, we understand that this might not be possible, so "No" is an acceptable answer. Papers cannot be rejected simply for not including code, unless this is central to the contribution (e.g., for a new open-source benchmark).
   - The instructions should contain the exact command and environment needed to run to reproduce the results. See the NeurIPS code and data submission guidelines (`https://nips.cc/public/guides/CodeSubmissionPolicy`) for more details.

- The authors should provide instructions on data access and preparation, including how to access the raw data, preprocessed data, intermediate data, and generated data, etc.
- The authors should provide scripts to reproduce all experimental results for the new proposed method and baselines. If only a subset of experiments are reproducible, they should state which ones are omitted from the script and why.
- At submission time, to preserve anonymity, the authors should release anonymized versions (if applicable).
- Providing as much information as possible in supplemental material (appended to the paper) is recommended, but including URLs to data and code is permitted.

6. **Experimental Setting/Details**

   Question: Does the paper specify all the training and test details (e.g., data splits, hyperparameters, how they were chosen, type of optimizer, etc.) necessary to understand the results?

   Answer: [Yes]

   Justification: We discuss the training and test details in the section on experiments.

   Guidelines:

   - The answer NA means that the paper does not include experiments.
   - The experimental setting should be presented in the core of the paper to a level of detail that is necessary to appreciate the results and make sense of them.
   - The full details can be provided either with the code, in appendix, or as supplemental material.

7. **Experiment Statistical Significance**

   Question: Does the paper report error bars suitably and correctly defined or other appropriate information about the statistical significance of the experiments?

   Answer: [Yes]

   Justification: We report the error and variance of predicted elevation and focal lens.

   Guidelines:

   - The answer NA means that the paper does not include experiments.
   - The authors should answer "Yes" if the results are accompanied by error bars, confidence intervals, or statistical significance tests, at least for the experiments that support the main claims of the paper.
   - The factors of variability that the error bars are capturing should be clearly stated (for example, train/test split, initialization, random drawing of some parameter, or overall run with given experimental conditions).
   - The method for calculating the error bars should be explained (closed form formula, call to a library function, bootstrap, etc.)
   - The assumptions made should be given (e.g., Normally distributed errors).
   - It should be clear whether the error bar is the standard deviation or the standard error of the mean.
   - It is OK to report 1-sigma error bars, but one should state it. The authors should preferably report a 2-sigma error bar than state that they have a 96% CI, if the hypothesis of Normality of errors is not verified.
   - For asymmetric distributions, the authors should be careful not to show in tables or figures symmetric error bars that would yield results that are out of range (e.g. negative error rates).
   - If error bars are reported in tables or plots, The authors should explain in the text how they were calculated and reference the corresponding figures or tables in the text.

8. **Experiments Compute Resources**

   Question: For each experiment, does the paper provide sufficient information on the computer resources (type of compute workers, memory, time of execution) needed to reproduce the experiments?

   Answer: [Yes]

   Justification: We train Era3D with 16 H800 GPUs.

   Guidelines:

   - The answer NA means that the paper does not include experiments.
   - The paper should indicate the type of compute workers CPU or GPU, internal cluster, or cloud provider, including relevant memory and storage.
   - The paper should provide the amount of compute required for each of the individual experimental runs as well as estimate the total compute.

- The paper should disclose whether the full research project required more compute than the experiments reported in the paper (e.g., preliminary or failed experiments that didn't make it into the paper).

9. **Code Of Ethics**

   Question: Does the research conducted in the paper conform, in every respect, with the NeurIPS Code of Ethics `https://neurips.cc/public/EthicsGuidelines`?

   Answer: [Yes]

   Justification: This work conforms with the NeurIPS Code of Ethics.

   Guidelines:

   - The answer NA means that the authors have not reviewed the NeurIPS Code of Ethics.
   - If the authors answer No, they should explain the special circumstances that require a deviation from the Code of Ethics.
   - The authors should make sure to preserve anonymity (e.g., if there is a special consideration due to laws or regulations in their jurisdiction).

10. **Broader Impacts**

    Question: Does the paper discuss both potential positive societal impacts and negative societal impacts of the work performed?

    Answer: [NA]

    Justification: There is no societal impact of the work performed.

    Guidelines:

    - The answer NA means that there is no societal impact of the work performed.
    - If the authors answer NA or No, they should explain why their work has no societal impact or why the paper does not address societal impact.
    - Examples of negative societal impacts include potential malicious or unintended uses (e.g., disinformation, generating fake profiles, surveillance), fairness considerations (e.g., deployment of technologies that could make decisions that unfairly impact specific groups), privacy considerations, and security considerations.
    - The conference expects that many papers will be foundational research and not tied to particular applications, let alone deployments. However, if there is a direct path to any negative applications, the authors should point it out. For example, it is legitimate to point out that an improvement in the quality of generative models could be used to generate deepfakes for disinformation. On the other hand, it is not needed to point out that a generic algorithm for optimizing neural networks could enable people to train models that generate Deepfakes faster.
    - The authors should consider possible harms that could arise when the technology is being used as intended and functioning correctly, harms that could arise when the technology is being used as intended but gives incorrect results, and harms following from (intentional or unintentional) misuse of the technology.
    - If there are negative societal impacts, the authors could also discuss possible mitigation strategies (e.g., gated release of models, providing defenses in addition to attacks, mechanisms for monitoring misuse, mechanisms to monitor how a system learns from feedback over time, improving the efficiency and accessibility of ML).

11. **Safeguards**

    Question: Does the paper describe safeguards that have been put in place for responsible release of data or models that have a high risk for misuse (e.g., pretrained language models, image generators, or scraped datasets)?

    Answer: [NA]

    Justification: The paper poses no such risks.

    Guidelines:

    - The answer NA means that the paper poses no such risks.
    - Released models that have a high risk for misuse or dual-use should be released with necessary safeguards to allow for controlled use of the model, for example by requiring that users adhere to usage guidelines or restrictions to access the model or implementing safety filters.
    - Datasets that have been scraped from the Internet could pose safety risks. The authors should describe how they avoided releasing unsafe images.
    - We recognize that providing effective safeguards is challenging, and many papers do not require this, but we encourage authors to take this into account and make a best faith effort.

12. **Licenses for existing assets**

Question: Are the creators or original owners of assets (e.g., code, data, models), used in the paper, properly credited and are the license and terms of use explicitly mentioned and properly respected?

Answer: [Yes]

Justification: This paper cites the related datasets and codes used in our work.

Guidelines:

- The answer NA means that the paper does not use existing assets.
- The authors should cite the original paper that produced the code package or dataset.
- The authors should state which version of the asset is used and, if possible, include a URL.
- The name of the license (e.g., CC-BY 4.0) should be included for each asset.
- For scraped data from a particular source (e.g., website), the copyright and terms of service of that source should be provided.
- If assets are released, the license, copyright information, and terms of use in the package should be provided. For popular datasets, `paperswithcode.com/datasets` has curated licenses for some datasets. Their licensing guide can help determine the license of a dataset.
- For existing datasets that are re-packaged, both the original license and the license of the derived asset (if it has changed) should be provided.
- If this information is not available online, the authors are encouraged to reach out to the asset's creators.

13. **New Assets**

Question: Are new assets introduced in the paper well documented and is the documentation provided alongside the assets?

Answer: [NA]

Justification: The paper does not release new assets.

Guidelines:

- The answer NA means that the paper does not release new assets.
- Researchers should communicate the details of the dataset/code/model as part of their submissions via structured templates. This includes details about training, license, limitations, etc.
- The paper should discuss whether and how consent was obtained from people whose asset is used.
- At submission time, remember to anonymize your assets (if applicable). You can either create an anonymized URL or include an anonymized zip file.

14. **Crowdsourcing and Research with Human Subjects**

Question: For crowdsourcing experiments and research with human subjects, does the paper include the full text of instructions given to participants and screenshots, if applicable, as well as details about compensation (if any)?

Answer: [NA]

Justification: The paper does not involve crowdsourcing or research with human subjects.

Guidelines:

- The answer NA means that the paper does not involve crowdsourcing nor research with human subjects.
- Including this information in the supplemental material is fine, but if the main contribution of the paper involves human subjects, then as much detail as possible should be included in the main paper.
- According to the NeurIPS Code of Ethics, workers involved in data collection, curation, or other labor should be paid at least the minimum wage in the country of the data collector.

15. **Institutional Review Board (IRB) Approvals or Equivalent for Research with Human Subjects**

Question: Does the paper describe potential risks incurred by study participants, whether such risks were disclosed to the subjects, and whether Institutional Review Board (IRB) approvals (or an equivalent approval/review based on the requirements of your country or institution) were obtained?

Answer: [NA]

Justification: The paper does not involve crowdsourcing nor research with human subjects.

Guidelines:

- The answer NA means that the paper does not involve crowdsourcing nor research with human subjects.
- Depending on the country in which research is conducted, IRB approval (or equivalent) may be required for any human subjects research. If you obtained IRB approval, you should clearly state this in the paper.
- We recognize that the procedures for this may vary significantly between institutions and locations, and we expect authors to adhere to the NeurIPS Code of Ethics and the guidelines for their institution.
- For initial submissions, do not include any information that would break anonymity (if applicable), such as the institution conducting the review.